GEOPHYSICAL RESEARCH LETTERS, VOL. 23, NO. 10, PAGES 1171-1174, MAY 15, 1996

Dispersion of regional body waves at 100-150 km depth beneath Alaska: In situ constraints on metamorphism of subducted crust

Geoffrey A. Abers and Golam Sarker

Department of Geology, University of Kansas, Lawrence

Abstract. Phase delays at high frequencies are observed in body waves that travel in the Alaska slab, along its strike at 100-150 km depth. The delays, between 2-6 Hz energy and the direct 0.5-1 Hz arrival, are 0.5-1.5 s for *P* waves and 1.5-4 s for *S* waves. Such dispersion suggests a waveguide structure that parallels the slab, perhaps near its top. A channel that is 2-6 km thick and 2.5-5% slower than surrounding mantle can explain the observations. The thickness of the layer is comparable to that of subducted oceanic crust or somewhat thinner. The layer may be crust that is slow at these depths. The required velocity anomaly is too small to be due to a continuous layer of metastable gabbro yet too large to represent an eclogite layer. It may indicate a mixture of the two, or persistence of hydrated mineral assemblages to depth.

Introduction

Many of the first-order changes to subducting plate properties occur at depths greater than 50-100 km, where high-resolution observations are difficult. A variety of changes in material properties may affect subducted oceanic crust as it descends through these depths (e.g. Helffrich et al., 1989; Kirby, 1995) which can lead to large structural variations over length scales of 5 km or less. Unfortunately, this length scale is nearly impossible to image through travel time tomography because of the great depth to the relevant zone; even the most detailed current velocity models (e.g. Zhao et al. 1994) do not resolve features smaller than 30-50 km.

To resolve these small-scale structures within the subducted plate, the frequency dependence of wave propagation is analyzed here. Several studies of propagation from Tonga events to New Zealand (e.g. Ansell and Gubbins, 1986; Gubbins and Snieder, 1991) have shown strong dispersion of *P* wave trains. There, high frequency (>1 Hz) energy tends to arrive up to 15 s earlier, for some paths, than does a dominant long period arrival. A contrasting observation has been made in central Honshu, where waves traveling up dip along the slab show high frequencies delayed by up to 1 s relative to the first long-period arrival (Iidaka and Mizoue, 1991). The location of ray paths, and the frequencies involved, suggest that dispersion is a signature of subducted oceanic crust or nearby lithosphere, which is expected to undergo a series of phase transformations as it descends. Still, the observed difference in behavior is difficult to interpret in terms of dry rheologies (Gubbins et al., 1994). In the present study we analyze dispersive behavior for propagation in a slab beneath Alaska and find dispersion similar to that seen in Japan, of a low-velocity waveguide. Delay times are then used to place constraints on phase assemblages present in subducted crust.

Paper number 96GL00974
0094-8534/96/96GL-00974$05.00

Observations

Data. We examine *P* waveforms for all events in the Alaska slab deeper than 100 km, for the years 1992 and 1993, recorded at Global Seismic Network station COL (Figure 1). These broadband records, recorded at 20 samples per second, have a flat instrument response to velocity at frequencies below 8 Hz. We use only waveforms with significant signal-to-noise levels at frequencies above 0.25 Hz, to resolve signal over a frequency span greater than one decade. This criterion gives 22 events at 300 to 800 km range from COL, where rays traverse the Alaska slab along strike, and 31 closer events from the region beneath Mt. McKinley where rays do not traverse the slab. All of these events are 100 – 170 km deep, and most are 100 – 120 km deep.

Rays and Arrival Times. In order to ascertain the nature of the first arrivals, travel times at COL are measured and com-

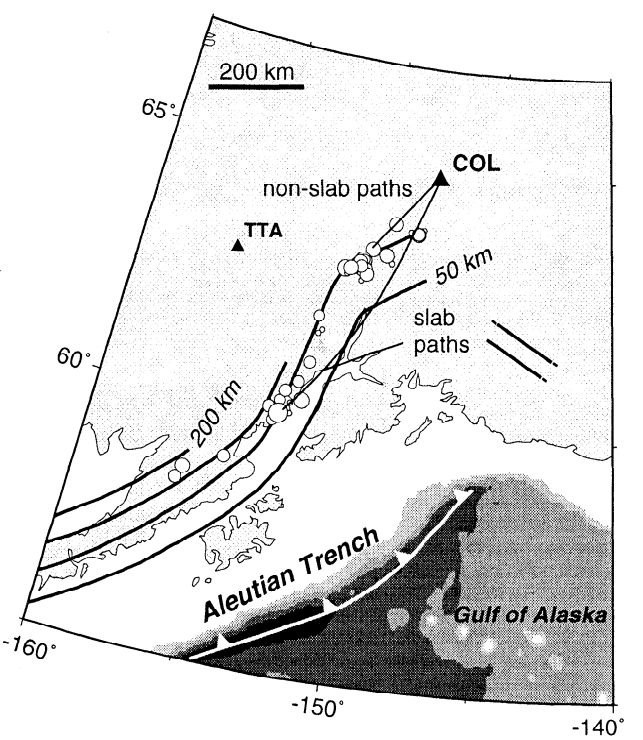

Figure 1. Map of Alaska slab, showing events used (circles, scaled to magnitude) and stations (triangles). Contours (thick lines) show depth to the Wadati-Benioff zone, from Page et al. (1989). Thin lines show examples of raypaths computed in the three-dimensional velocity structure.

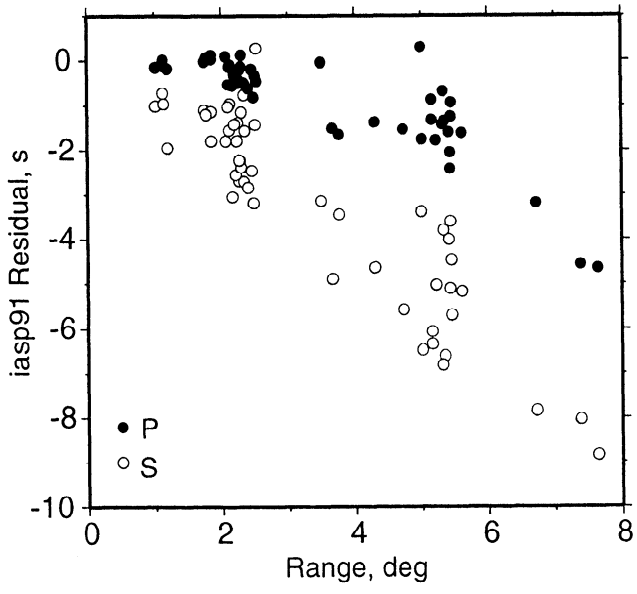

Figure 2. Measured arrival time residuals for *P* waves (dark circles) and *S* waves (light circles) traveling along the Alaska slab to COL from 100-150 km deep events, relative to the *iasp91* travel time curves (Kennett and Engdahl, 1991). Times correspond to the first, low-frequency arrival.

pared to a one-dimensional Earth model (Kennett and Engdahl, 1991). Observed arrivals are early, increasingly so beyond 100-200 km distance (Figure 2). Residuals increase with distance, and are 4-5 s at 8° for *P* arrivals and 8-9 s for *S*, consistent with a slab that is 5-8% fast. *P* and *S* show similar relative travel time perturbations.

Raypaths from these events are traced through a three-dimensional slab model, which is 75 km thick and whose top follows the contours of Page et al. (1989). The interior is assumed to be 5% or 8% fast at its core. The values bound those that we found to be consistent with arrival times, and includes the 5% fast slab found by Zhao et al. (1995). Rays are traced through a three-dimensional mesh of tetrahedra by an exact shooting method (Roecker, 1989; Abers, 1994). These forward calculations (Figure 1) show that rays from events south of 62°N travel within the slab along its strike, to where it bends at 64°N. Because of the unusual geometry, seismic signals sample only that part of the slab between 100 and 150 km depth but remain in the slab for several hundred kilometers.

Dispersion. Seismograms from close "non-slab" paths that immediately exit the slab show impulsive *P* waves (Figure 3, left). By contrast, records from paths that follow the slab are dispersed and show an initial low-frequency arrival followed later by high-frequency signal (Figure 3, right). Similar behavior is observed for *S* waves. Presumably, short wavelength signals follow a low velocity path that is too small for long wavelength signals to sample.

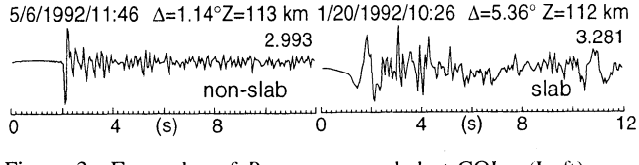

Figure 3. Examples of *P* waves recorded at COL. (Left) samples a path that does not sample the slab, and is impulsive. (Right) samples the slab for ~300 km, and shows dispersion analyzed in Fig. 4. Peak amplitudes, in μm s^{-1}, shown on right of each record.

This *P* wave dispersion is quantified by examining the group arrival time variations with frequency. At a series of frequency intervals between 0.75 and 6 Hz the vertical-component *P* seismograms are band-passed using 6-pole zero-phase filters (Figure 4, left). The narrow-band records are squared and averaged with a Gaussian-weighted RMS smoothing operator, with a 0.5s half-width (Figure 4, right). The timing of the peaks in these smoothed, rectified envelopes is picked as an estimate of group arrival time for dispersive waves. The resulting dispersion curve is corrected to a reference zero dispersion at 0.75 Hz. A similar approach is often used to measure surface-wave group velocities (Dziewonski et al., 1969).

One of two patterns are seen from this analysis (Figure 5). "Non-slab" records, sampling ~100-250 km long paths to COL, display near-zero delays for all frequencies. However, "slab" records, for raypaths that travel more than 150 km within the slab, show that signals at frequencies above 2-3 Hz are delayed relative to 0.5-2 Hz arrivals. Delays are near 1 s for paths with 150-300 km long segments in the slab. We also examined records for some of the same events recorded at stations in the Alaska regional network (e.g. Page et al., 1989). Long raypaths that depart the slab or rays that depart the slab immediately, such as to TTA (Figure 1), show no significant dispersion. Hence, dispersion is only associated with slab paths.

Amplitudes. Amplitudes are also high at high frequencies (Figures 3, 4). This is unexpected, because waveforms sampling backarc paths often show significant attenuation at these depths (e.g. Bowman, 1988). The slab path, besides being dispersive, must be an efficient propagator of high-frequency energy. High amplitudes are observed for both *P* and *S*, so the physical structure of the waveguide region cannot be one that attenuates either wave type. High frequency amplification is enhanced by Airy phase behavior (a minimum in group velocity curves) associated with wave guides, as high-frequency energy is channeled along the wave guide.

Discussion

The apparent dispersion seen for slab paths suggests that a wave guide or other frequency-dependent multipathing effect

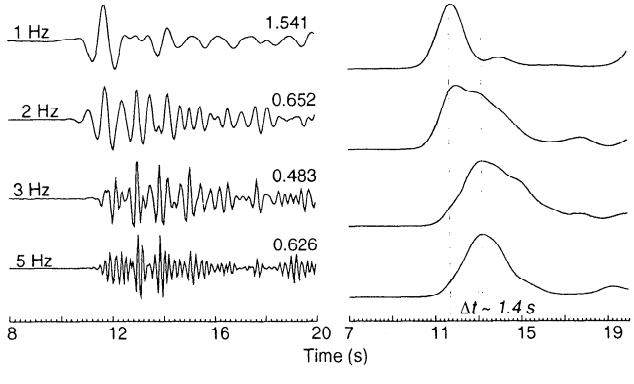

Figure 4. Example of dispersion analysis for a slab waveform (raw record on Fig. 3, right). (Left) narrow-band-filtered waveforms. Amplitudes corrected to μm s^{-1} are shown to upper right of each record, passband is shown upper left in Hz. (Right) smoothed envelopes from which group delays are measured. In this example, a 1.40 s delay is measured at 5 Hz.

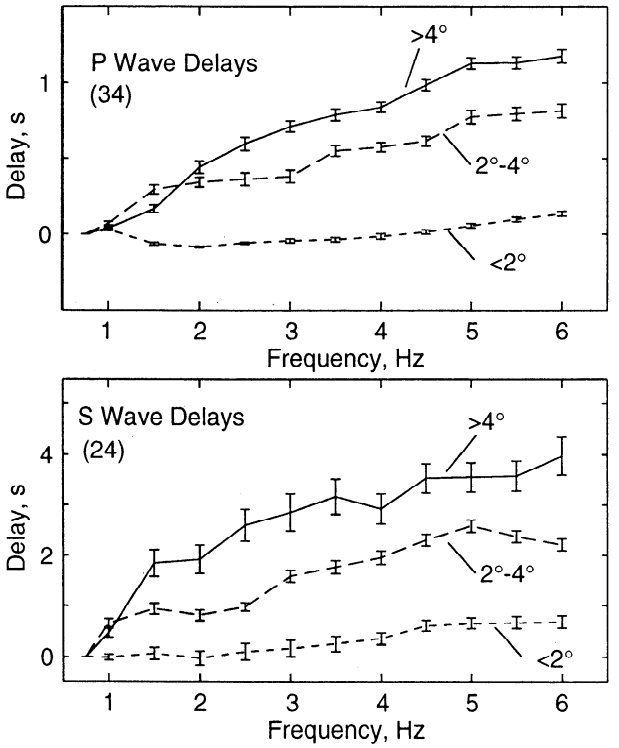

Figure 5. Dispersion curves, for P (top) and S (bottom), averaged over three distance ranges. Time delays are relative to 0.75 Hz. Error bars are one-sigma standard deviations of the mean. The number of records used in each average is also listed. Dispersion increases with increasing distance, labeled.

occurs near the top of the subducting plate, much as is observed in Japan. Several alternative possibilities can be ruled out. First, scattering and multipathing in upper-plate crust beneath the station is unlikely, as waveforms from non-slab events which have approximately the same back-azimuth and incidence angle do not show these effects. Second, unusual source variations are probably not responsible, as similar dispersion is seen for waveforms varying ~100 times in signal amplitude, and for the same event dispersion is not seen at all regional-network stations. Third, other phases, predicted by radially stratified models, are not expected. Reflections off the 410- or 670-km discontinuities would arrive 15-30 s too late, and refractions or phase conversion off the free surface or Moho would arrive at least 10 s after P. Fourth, simple phase conversions off a slab-mantle interface (e.g., Iidaka and Mizoue, 1991) can not explain the frequency dependence and amplitude behavior of the later phases.

High-frequency phase delays are characteristic of scattering media (e.g. Richards and Menke, 1983) and scattering may play a significant role within the slab. Indeed, the slab-guided waves show significantly more coda excitation than the non-slab waves, so increased scattering is suspected. We attempted to simulate the dispersion caused by scattering using two-dimensional finite-difference acoustic wavefield calculations (Keiswetter et al., 1996). Although these experiments can produce dispersion comparable to that observed, they require a 10-20% velocity variation at 0.5-1 km scales both along and across the slab, over a region several times thicker than subducted crust. Such 10-20% velocity variations at ≤1 km scales could be caused by retention of ~4% fluid or melt by volume (Helffrich et al., 1989) or by differences in behavior of fine-grained basalt and coarse-grained gabbro (Hacker, 1996). However, it seems likely that such large variations will be present only across the strike of the slab, not laterally within it, so to first order we consider one-dimensional wave guides as adequate to explain the dispersion.

Waveguide effects. The dispersive behavior of body waves traveling in the slab resembles that due to a buried waveguide. For simple waveguide geometries, such as a planar channel, high frequencies are expected to travel at the channel velocity while low frequencies will travel at the velocity of the surrounding medium. A first estimate of waveguide dimensions is made by visually inspecting dispersion curves for a characteristic frequency. In cases where the P-wave phase delay increases abruptly with frequency (Figure 4), the transition frequency between fast and slow arrivals is between 1.5 to 3 Hz. These frequencies correspond to 2.5-5.5 km wavelengths at nominal mantle velocities and can be considered nominal layer thicknesses.

A second estimate is made by comparing observed dispersion to analytical expressions for waveguide dispersion in a constant-velocity layer buried in a uniform medium. We calculate fundamental-mode dispersion for a low-velocity acoustic channel from analytical solutions to the buried layer problem, following the derivations of Gubbins and Snieder (1991). These solutions can give estimates of group velocity as a function of frequency. The predicted group delay time is controlled by two quantities -- the ratio of layer thickness to velocity, which controls the frequency behavior, and the slowness perturbation of the layer multiplied by the path length, which controls the amplitude of the time delay.

A grid search is used to determine the layer thickness and velocity that best explains the observations (Figure 5) using this acoustic theory. The RMS difference between predicted delays and those observed in the dispersion curves is minimized simultaneously for all observations. In these calculations, the last 220 km of propagation is assumed to occur outside the waveguide and we only fit raypaths longer than 300 km. The channel thicknesses are weakly constrained by this fitting procedure to 2.4 km for P and 1.9 km for S (for nominal 8 km/s mantle P velocity), and have uncertainties of 1-3 km for a variety of weighting schemes and statistical treatments. The inferred velocity perturbations, 2.6% for P and 4.5% for S, have uncertainties near 1%. Within the uncertainties P and S show similar behavior. Because many of the dispersion curves clearly show effects at frequencies below 3 Hz (wavelength of 2.7 km) channels thinner than 2-3 km do not seem realistic. Synthetic seismograms for the same structure generated in a fully elastic finite-difference calculation, not shown here, show similar dispersion to that observed. Hence, a range of 2-5.5 km for channel thickness and velocity perturbations of 1.5-4% (3-6% for S) are most consistent with the data.

Implications and Conclusions

In equilibrium conditions, dry gabbroic crust should convert to eclogite at depths of 20-30 km (Ahrens and Schubert, 1975). Eclogite is 15-20% denser and faster than gabbro and should have seismic velocities that are close to or exceeding that of the surrounding mantle (Helffrich et al., 1989; Gubbins et al., 1994), so should not create a low velocity anomaly. However, there has long been suspicion that these reactions may be too sluggish at slab temperatures (Ahrens and Schubert, 1975), and several studies of wave effects beneath

Japan have argued that gabbro persists to great depth (e.g. Hori et al., 1985). The observations here, of 1.5-4% slow waveguides at 100-150 km depth, are difficult to reconcile with either endmember composition, unconverted gabbro or dry eclogite, and may indicate either an intermediate mix or hydrated compositions.

Recently, several scenarios have been proposed by which water affects phase stability and reaction rate. Devolatilization might be necessary to generate eclogite (Kirby, 1995) so that the reaction happens from 70 to 150 km depth. If temperatures are low blueschists (hydrous metamorphic assemblages) may be stable at high pressure and could produce a layer 4-10% slower than surrounding mantle (Peacock, 1993; Helffrich, 1996). Observations of stable lawsonite blueschist to >6 GPa and >800°C (Poli and Schmidt, 1995) confirm the viability of this scenario. Suggestions that the basaltic upper crust may transform at significantly faster rates than the gabbroic lower crust (Hacker, 1996) may explain why the inferred waveguide (2-5.5 km thick) is somewhat thinner than oceanic crust (5-8 km).

Alternatively, the mantle wedge immediately above the downgoing plate may become hydrated as water is freed, which would result in a low-velocity serpentinized zone (Meade and Jeanloz 1991). Abundant free water is difficult to reconcile with seismic observations, however, as the waveguide must have low attenuation in order to propagate high-frequency energy efficiently. Before this possibility can be fully evaluated, more quantitative predictions of the nature and dimensions of a serpentinized zone are needed.

In summary, pronounced dispersion of body waves that follow slabs suggest significant structure at 2-6 km length scales. The dispersion seen in Alaska, similar to that in Japan, implies a low-velocity wave guide that likely reflects subduction of oceanic crust in some way. Although several possibilities exist, the observations require a 2.5-5% slow channel that is fairly contiguous along the length of the slab, at least at 100-150 km depth. Such a zone is not slow enough to be comprised of metastable gabbro, although a mixture including regions of gabbro metastability are possible. Hydrous phases, either in the subducted crust or in the adjacent mantle, may provide viable alternatives.

Acknowledgments. Data from global network stations were made available by the IRIS Data Management Center. We thank C. Rowe for providing seismograms from the Alaska Network seismograms for selected events. The text benefited from useful reviews by B. Hacker, G. Helffrich, and G. Smith. Partial publication costs and method development funded by AFOSR grant F49620-95-0002.

References

Abers, G.A., Three-dimensional inversion of regional *P* and *S* arrival times in the East Aleutians and sources of subduction zone gravity highs, *J. Geophys. Res.*, *99*, 4395-4412, 1994.

Ahrens, T.J. and G. Schubert, Gabbro-eclogite reaction rate and its geophysical significance, *Rev. Geophys. Space Phys.*, *13*, 383-400, 1975.

Ansell, J.H., and D. Gubbins, Anomalous high-frequency wave propagation from the Tonga-Kermadec seismic zone to New Zealand, *Geophys. J. R. Astr. Soc.*, *85*, 93-106, 1986.

Bowman, J. R., 1988, Body wave attenuation in the Tonga subduction zone: *J. Geophys. Res.*, *93*, 2125-2139.

Dziewonski, A., S. Bloch and M. Landisman, A technique for the analysis of transient seismic signals, *Bull. Seism. Soc. Am.*, *59*, 427-444, 1969.

Gubbins, D., A. Barnicoat, and J. Cann, Seismological constraints on the gabbro-eclogite transition in subducted oceanic crust, *Earth and Planet. Sci. Lett.*, *122*, 89-101, 1994.

Gubbins, D., and R. Snieder, Dispersion of *P* waves in subducted lithosphere: Evidence for an eclogite layer, *J. Geophys. Res.*, *96*, 6321-6333, 1991.

Hacker, B.R., Eclogite formation and the rheology, buoyancy, seismicity and H_2O content of oceanic crust, in *Dynamics of Subduction, Geophysical Monograph*, edited by G.E. Bebout, D. Scholl, and S. Kirby, AGU, Washington, D.C., in press, 1996.

Helffrich, G. R., S. Stein and B. J. Wood, Subduction zone thermal structure and mineralogy and their relationship to seismic wave reflections and conversions at the slab/mantle interface, *J. Geophys. Res.*, *94*, 753-763, 1989.

Helffrich, G., Subducted lithospheric slab velocity structure: Observations and mineralogical inferences, in *Dynamics of Subduction, Geophysical Monograph*, edited by G.E. Bebout, D. Scholl, and S. Kirby, AGU, Washington, D.C., in press, 1996.

Hori, S., H. Inoue, Y. Fukao and M. Ukawa, Seismic detection of the untransformed "basaltic" oceanic crust subducting into the mantle, *Geophys. J. R. Astr. Soc.*, *83*, 169-197, 1985.

Iidaka, T, and M. Mizoue, P-wave velocity structure inside the subducting Pacific plate beneath the Japan region, *Phys. Earth Planet. Int.*, *66*, 203-213, 1991.

Keiswetter, D., Black, R.A., and Schmeissner, C., in press, FINMODEL.FOR: A program for seismic wavefield modeling using finite-difference techniques, *Computers and Geosciences*, in press, 1996.

Kennett, B.L.N., and E.R. Engdahl, Travel times for global earthquake location and phase identification, *Geophys. J. Int.*, *105*, 429-465, 1991.

Kirby, S., Intraslab earthquakes and phase changes in subducting lithosphere, US National Report to IUGG 1991-1994, *Rev. Geophys., suppl.*, 287-297, 1995.

Meade, C., and R. Jeanloz, Deep-focus earthquakes and recycling of water into the Earth's mantle, *Science*, *252*, 68-72, 1991.

Page, R.A., C.D. Stephens and J.C. Lahr, Seismicity of the Wrangell and Aleutian Wadati-Benioff zones and the North America plate along the Trans-Alaska crustal transect, Chugach mountains and Copper River basin, southern Alaska, *J. Geophys. Res.*, 94, 16059-16082, 1989.

Peacock, S.M., The importance of blueschist -> eclogite dehydration in subducting oceanic crust, *Geol. Soc. Am. Bull.*, *105*, 684-694, 1993.

Poli, S. and M.W. Schmidt, H_2O transport and release in subduction zones: Experimental constraints on basaltic and andesitic systems, *J. Geophys. Res.*, *100*, 22,299-22,314, 1995.

Richards, P.G., and W. Menke, The apparent attenuation of a scattering medium, *Bull. Seism. Soc. Am.*, *73*, 1005-1021, 1983.

Roecker, S.W., Determination of earthquake hypocenters, focal mechanisms, and velocity structures in the Morgan Hill/Coyote Lake and Bear Valley/Stone Canyon areas of Central California through the use of fast, accurate three-dimensional ray tracing, *USGS Open File Report*, *89-453*, 99, 1989.

Zhao, D., A. Hasegawa and H. Kanamori, Deep structure of Japan subduction zone as derived from local, regional, and teleseismic events, *J. Geophys. Res.*, *99*, 22,313-22,330, 1995.

Zhao, D., D.H. Christensen, and H. Pulpan, Tomographic imaging of the Alaska subduction zone, *J. Geophys. Res.*, 100, 6487-6504, 1995.

G. Abers, G. Sarker. Department of Geology, 120 Lindley Hall, University of Kansas, Lawrence, KS 66045; g-

(Received December 14, 1995; accepted February 13, 1996)